Theory of the adatom-induced reconstruction of the SiC(0001)$\sqrt{3} \times \sqrt{3}$ surface

John E. Northrup and J. Neugebauer

Xerox Palo Alto Research Center, 3333 Coyote Hill Road, Palo Alto, California 94304

Based on first-principles total-energy calculations we have determined the chemical identity and adsorption site of the adatoms observed recently in scanning tunneling microscopy on the SiC(0001)$\sqrt{3} \times \sqrt{3}$ surface. The calculations indicate that Si adatoms are preferred over C adatoms for the entire allowed range of Si and C chemical potentials. In addition, we find that the adatoms prefer the T_4 site over the H_3 site for both Si and C. Based on these results we propose a model for the C-rich $6\sqrt{3} \times 6\sqrt{3}$ reconstruction.

Silicon carbide (SiC) is a wide-band-gap semiconductor manifesting a large number of polytypes including the $3C$ (zinc-blende), $2H$ (wurtzite), and $6H$ structures. These structures exhibit similar local atomic structures, differing mainly in the stacking sequence of Si-C double layers. Having a lattice mismatch of -3.5% with GaN, SiC has emerged as a very useful substrate for the growth of nitride-based optoelectronic device structures.[1] For this and other reasons, it is important to characterize the stoichiometry and structure of its surfaces.

The (111) surface of the $3C$ polytype and the (0001) surface of the $6H$ polytype have been examined by Kaplan[2] with low-energy electron diffraction (LEED). In each polytype Kaplan observed both the 3×3 and $\sqrt{3} \times \sqrt{3}$ reconstructions. Moreover, the LEED patterns for the corresponding reconstructions on the $3C$-(111) and the $6H$-(0001) surfaces were found to be essentially identical, making it likely that the surface reconstructions for the two polytypes are the same. Given the structural similarity between the polytypes this is not surprising. In fact, the stacking sequence of $6H$ and $3C$ are the same down to at least four layers from the surface. Kaplan conjectured that the 3×3 reconstruction might correspond to additional layers of Si configured in a dimer–adatom–stacking-fault arrangement atop a Si-terminated double layer of SiC. The 3×3 phase is more Si rich than the $\sqrt{3} \times \sqrt{3}$ phase and the latter can be prepared by annealing the 3×3 phase at 950 °C. Based on structural determinations made for group-III elements[3] on the Si(111) surface, Kaplan suggested the possibility of an adatom model for the $\sqrt{3} \times \sqrt{3}$ phase. At annealing temperatures greater than 1150 °C, the surface adopts a $6\sqrt{3} \times 6\sqrt{3}$ reconstruction, which is associated with graphitization of the surface.[4]

In a recent scanning tunneling microscope (STM) study Owman and Martensson[5] have examined the surface of the Si-terminated (0001) face of the $6H$ phase. They observed a well-ordered $\sqrt{3} \times \sqrt{3}$ array of protrusions that they identified as adatoms. However, the STM data did not distinguish between Si and C adatoms, and it was not possible to determine the adsorption site of the adatoms: T_4 or H_3. In this work we report the results of first-principles total-energy calculations for SiC surfaces which allow us to determine the relative energetics and local atomic structure of intrinsic adatom-induced $\sqrt{3} \times \sqrt{3}$ structures. We find that Si adatoms are strongly bound to the Si-terminated surface and are fa-

vored energetically over C adatoms for all possible chemical potentials of Si and C. These results indicate that the adatom-induced $\sqrt{3} \times \sqrt{3}$ reconstruction on SiC(0001) consists of Si adatoms occupying T_4 sites.

The surface of SiC was modeled in the supercell approach with 12 layers of SiC. In the interior of the slab the stacking sequence was taken to be zinc blende. On one side of the slab the dangling bonds on the carbon atoms were saturated with H atoms. On the Si-terminated surface we placed Si (or C) adatoms in the threefold-symmetric T_4 or H_3 sites as indicated schematically in Fig. 1. For each one of these four models the atomic positions of the adatoms and the first four layers of the SiC substrate were allowed to relax. The total-energy calculations were performed using the density-functional method and employed the exchange and correlation energy function derived by Perdew and Zunger[6] from the Ceperley and Alder electron-gas data. Forces and total energies were determined using an optimized version of the plane-wave code similar to that described by Stumpf and Scheffler.[7] In this approach the pseudopotentials are expressed in the form due to Kleinman and Bylander.[8] To minimize the number of plane waves needed in the calculation we employed a soft pseudopotential for C which was generated according to the scheme of Troullier and Martins.[9] For Si we employed the pseudopotential described by Gonze *et al.*[10] As discussed below, with a plane-wave cutoff of 40 Ry these pseudopotentials provide an accurate description of the bulk structural properties of C, Si, and SiC as well as an accurate heat of formation for SiC. For the surface calculations the plane-wave cutoff was taken to be 40 Ry and six k points were used to sample the irreducible $\sqrt{3} \times \sqrt{3}$ Brillouin zone.

For both Si and C adatoms we found the T_4 site to be preferred energetically: for Si adatoms the energy difference is 0.54 eV/($\sqrt{3} \times \sqrt{3}$) and for C the energy difference is 0.32 eV/($\sqrt{3} \times \sqrt{3}$). This adsorption site is also the most favorable for Si, Al, In, and Ga adatoms on the Si(111) surface.[3]

For the T_4 structure [Fig. 1(a)], the bond length between the Si adatom and the first-layer Si atoms is calculated to be 2.42 Å. This is slightly larger than twice the covalent radius of Si ($r_{Si} = 1.17$ Å, $r_C = 0.77$ Å). The corresponding C-Si bond length in the C adatom model is 1.98 Å, a value that is again only slightly larger than the sum of radii for Si and C ($r_{Si} + r_C = 1.94$ Å). The atomic relaxations induced in
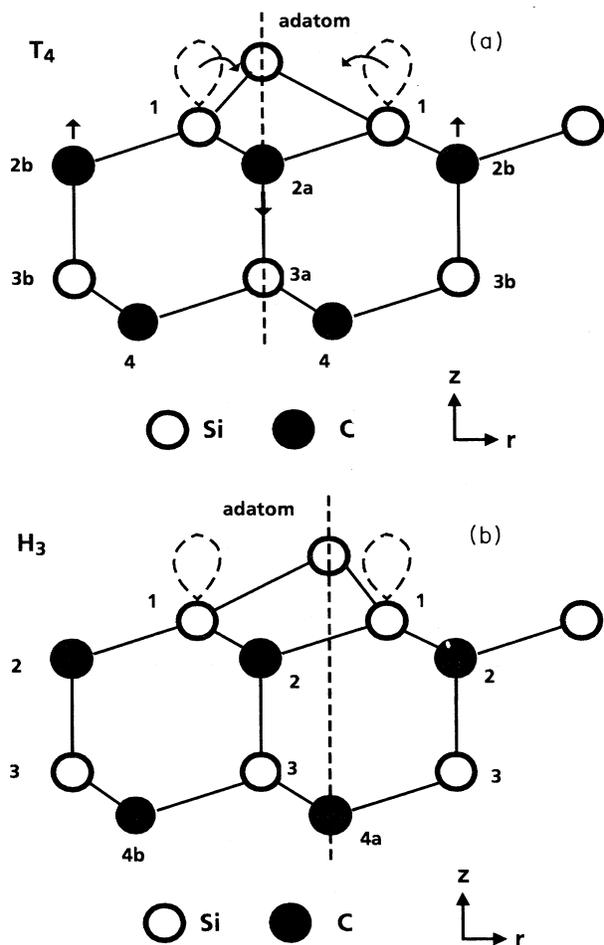
FIG. 1. (a) Schematic representation of the T_4 adatom model. (b) Schematic represenation of the H_3 adatom model. Substrate relaxations are listed in Tables I and II. The dashed line indicates a threefold axis of symmetry passing through the adatom. In the T_4 structures the vertical buckling in the second layer ($2a$ moves up and $2b$ moves down) rotates the dangling bonds on the Si towards the adatom.

the substrates by the adatoms are given in Table I. We find that the adatoms induce large vertical displacements in the SiC substrate but that these adatom-induced displacements are significantly less for Si adatoms than for C adatoms. For example, $z_{2a}-z_{2b}= -0.22$ Å for the Si adatom model and -0.52 Å for the C adatom model. The vertical separation between the adatom and the first layer is much less for the C adatom than for the Si adatom; $z_{C\,adatom}-z_1 = 1.22$ Å and $z_{Si\,adatom}-z_1 = 1.75$ Å for Si. Because the atomic radius of C is much smaller than that of Si, to form bonds the C adatom moves closer to the substrate and therefore induces a larger elastic response. Atomic displacements calculated for the H_3 models are listed in Table II. Here we find that the substrate relaxations are mainly lateral and again we see that C adatoms induce larger relaxations than Si.

The greater stability of the T_4 structure arises in part from the increased hybridization between the substrate dangling bonds and the p orbitals of the adatom. The symmetry of the T_4 structure allows vertical buckling of the second-layer at-

TABLE I. Atomic displacements in Å for the Si- and C-T_4 adatom structures. Atom numbers refer to Fig. 1. δr is the lateral relaxation of the atoms towards ($\delta r<0$) or away ($\delta r>0$) from the threefold axis passing through the adatom. δz is the displacement in the (111) direction.

| Atom | Si-T_4 | | C-T_4 | |
	δz	δr	δz	δr
1 (Si)	0.02	-0.06	0.08	-0.18
$2a$ (C)	-0.14	0.0	-0.27	0.0
$2b$ (C)	0.08	0.0	0.25	0.0
$3a$ (Si)	-0.07	0.0	-0.15	0.0
$3b$ (Si)	0.03	0.0	0.09	0.0
4 (C)	0.00	0.01	0.06	0.03

oms, which is prohibited in the H_3 structure. As indicated schematically in Fig. 1(a), this buckling rotates the dangling bonds of the first-layer atoms so that they point more directly at the adatom, and this increases the strength of the bonds between the adatom and the first-layer Si atoms.

To address the issue of whether the adatoms observed by Owman and Martensson[5] are Si or C, we introduce chemical potentials as discussed in previous work.[11,12] The energy of the Si-terminated and C-terminated surfaces, expressed relative to that of the ideal Si-terminated 1×1 surface, is dependent on the chemical potentials of Si and C:

$$\Delta E = \Delta E_{Si\,rich} + \Delta n(\mu_{Si} - \mu_{Si(bulk)}).$$

In this expression Δn is the difference in the number of carbon and silicon atoms per $\sqrt{3}\times\sqrt{3}$ unit cell. Thus $\Delta n = -1$ for the Si adatom surface and $+1$ for the C adatom surfaces. The chemical potential of Si (μ_{Si}) varies within a range determined by the chemical potential of bulk Si and the heat of formation of SiC: $\mu_{Si(bulk)} - \Delta H < \mu_{Si} < \mu_{Si(bulk)}$. Thus the formation energy of the Si adatom surface decreases by the heat of formation of SiC (ΔH) as one passes from the C-rich limit, $\mu_{Si} = \mu_{Si(bulk)} - \Delta H$, to the Si-rich limit, $\mu_{Si} = \mu_{Si(bulk)}$. To determine ΔH we performed total-energy calculations for bulk phases of Si, C, and SiC. These calculations employed the diamond structure for Si and C, and the zinc-blende structure for SiC. Of course, the bulk phase of C that would limit the chemical potential is most likely graphite.[4] However, it is known experimentally[13] that the chemical potential of diamond is only slightly higher than that of graphite. The difference is approximately 0.02

TABLE II. Atomic displacements in Å for the Si- and C-H_3 adatom structures. Atom numbers refer to Fig. 1. δr is the lateral relaxation of the atoms towards ($\delta r<0$) or away ($\delta r>0$) from the threefold axis passing through the adatom. δz is the displacement in the (111) direction.

| Atom | Si-H_3 | | C-H_3 | |
	δz	δr	δz	δr
1 (Si)	0.02	-0.05	0.00	-0.16
2 (C)	0.00	0.05	0.00	0.12
3 (Si)	0.00	0.02	0.00	0.04
$4a$ (C)	0.03	0.0	0.04	0.0
$4b$ (C)	0.00	0.0	-0.04	0.0
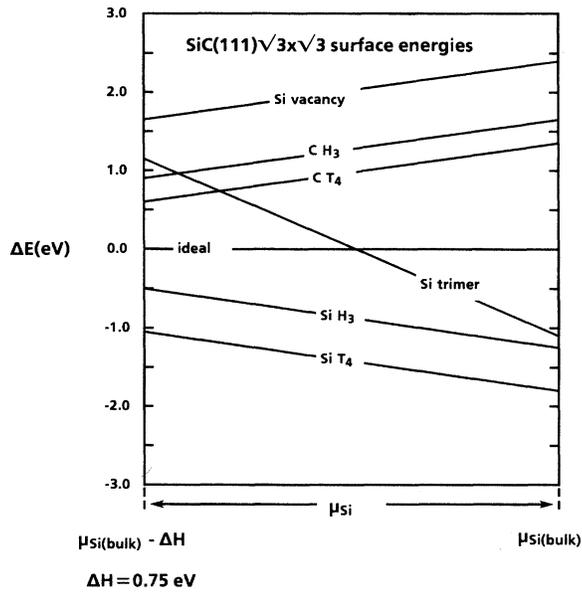
FIG. 2. Formation energies for various possible $\sqrt{3} \times \sqrt{3}$ surfaces of SiC. The formation energies are given relative to that of the ideal Si-terminated surface of SiC. The Si-T_4 adatom model is energetically favorable with respect to the other structures over the entire allowed range of the Si chemical potential.

FIG. 3. Electronic structure calculated for the Si-T_4 adatom model. Excitation energies are given relative to the bulk valence-band maximum (VBM). The Σ_1 band is half filled and the Fermi energy is located 1.2 eV above the VBM.

eV/atom, which is negligibly small for the purposes of the present studies. We are therefore justified in employing the diamond structure in calculations to determine the maximum chemical potential of C. For each of these bulk calculations the k-point sampling scheme employed 10 k points and the plane-wave cutoff was 40 Ry. The theoretical lattice constant determined by energy minimization was found to be (in Å) 5.38 for Si, 3.53 for C, and 4.30 for SiC. These results are in close agreement with the experimental values:[14] 5.43 for Si, 3.56 for C, and 4.36 Å for SiC. The theoretical heat of formation, $\Delta H = 0.75$ eV, is in good agreement with the experimental value $\Delta H_{expt} = 0.72$ eV.[13]

Results for the Si and C adatom-induced reconstructions together with results for the ideal surface, a Si trimer structure, and a Si vacancy structure are shown in Fig. 2. We see that over the entire range of allowed chemical potentials the Si-T_4 adatom structure is preferred. Its energy is lower than the ideal surface by 1.8 eV/cell in the Si-rich limit and by 1.05 eV/cell in the C-rich limit. Even in the C-rich limit, the C adatom models are quite high in energy relative to both the Si adatom and the ideal surface. From these results it is clear that the $\sqrt{3} \times \sqrt{3}$ phase corresponds to the Si adatom model. The C atom is simply too small to saturate efficiently the dangling bonds of the first-layer Si atoms.

The possibility that each protrusion observed in the STM images could correspond to a Si trimer was noted by Owman and Martensson.[5] We tested the possibility of a Si trimer centered over the T_4 site of SiC and found that under Si-rich conditions its energy is still 0.7 eV/cell higher than the Si-T_4 adatom structure. Therefore we may safely rule out the possibility of Si trimers as an equilibrium phase on SiC. Calculations were also performed for a $\sqrt{3} \times \sqrt{3}$ vacancy structure. Vacancy creation in the surface layer exposes three
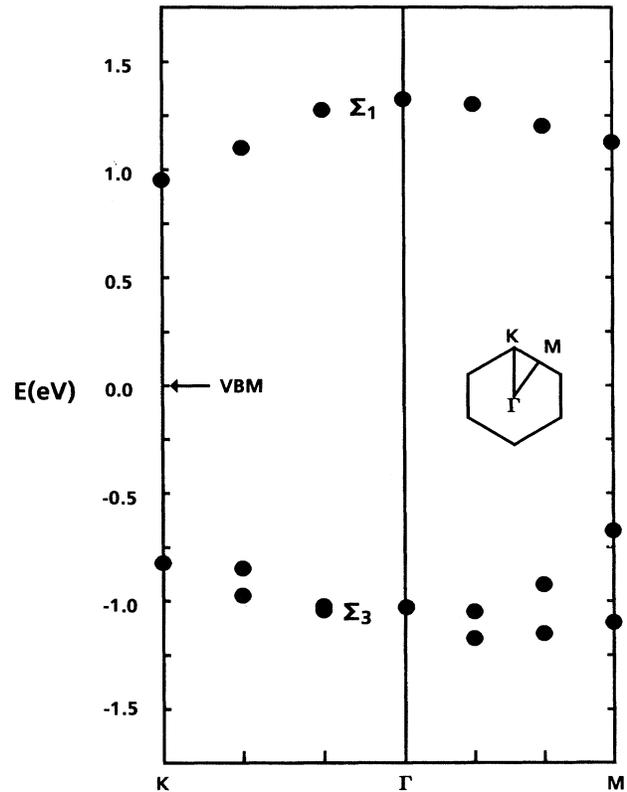
dangling bonds on the second-layer C atoms. As seen in Fig. 2, vacancy formation is energetically unfavorable.

The surface-state band structure calculated for the Si-T_4 model is shown in Fig. 3. The band labeled Σ_1 is derived from dangling bonds on the Si adatoms and the two bands labeled Σ_3 are derived from the p_x and p_y orbitals of the adatoms, which are coupled to the substrate dangling bonds. Contour plots of the Σ_3 and Σ_1 states are shown in Fig. 4. The two Σ_3 bands are degenerate at the Γ and K points and the energy splitting is 0.47 eV at the M point. In our local-density-approximation calculations the Σ_1 band is centered about 1.2 eV above the bulk valence-band maximum and has a width of 0.35 eV. In a single-particle picture, the Σ_1 band is
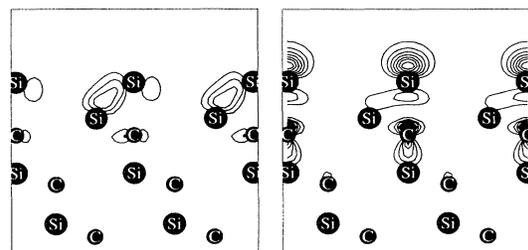
FIG. 4. Σ_3 and Σ_1 surface electronic states at the Γ point for the Si-T_4 adatom model.

half filled. It is very likely that the state that is imaged in the STM experiments is the Σ_1 surface state. This is consistent with the fact that the STM images are similar for tunneling in and out of the surface.[5]

The existence of a half-filled dangling-bond-derived band would seen to be an exception to the electron counting rule. According to this rule the reconstructions that give rise to a metallic occupation are energetically unfavorable with respect to at least one reconstruction for which a semiconducting occupation can be obtained. However, this rule is by no means universal. For example, a half-filled Σ_1 band has been observed for the Si(111)$\sqrt{3} \times \sqrt{3}$:Sn structure, which has $\frac{1}{3}$ ML of Sn adatoms on the Si(111) surface.[15] It should be pointed out that in view of the narrowness of the Σ_1 band it is conceivable that correlation effects beyond the scope of a one-electron theory are important. It would therefore be interesting to probe the Σ_1 band dispersion with photoemission and inverse-photoemission experiments, and also to perform local spectroscopy on the adatom with the STM to characterize the electronic structure near the Fermi level.

Chang et al.[4] have characterized the $6\sqrt{3} \times 6\sqrt{3}$ reconstruction that occurs at higher annealing temperatures and have shown it to be associated with graphitization of the surface. They suggested that this reconstruction corresponds to a monolayer of graphite atop a 1×1 SiC surface. Given our result that the Si-T_4 adatom model is very stable with respect to the ideal surface even under conditions that lead to the precipitation of graphite, we propose instead that the $6\sqrt{3} \times 6\sqrt{3}$ structure arises from a monolayer of graphite resting above and interacting weakly with the $\sqrt{3} \times \sqrt{3}$ array of Si adatoms. The in-plane lattice constant of bulk graphite is 2.456 Å.[16] This may be compared with the lattice constant required for a 13×13 graphite cell to match exactly a $6\sqrt{3} \times 6\sqrt{3}$ cell of SiC. The required lattice constant is 2.464 Å. Therefore there should be very little stress in a weakly interacting graphite monolayer that is in registry with a $6\sqrt{3} \times 6\sqrt{3}$ SiC substrate.

In conclusion, we have shown that over the entire range of thermodynamically allowed chemical potentials Si adatoms are preferred over C adatoms on the SiC(111) $\sqrt{3} \times \sqrt{3}$ surface, and that the adatoms prefer the T_4 site. For the Si-T_4 model there is a half-filled adatom dangling-bond band located approximately 1.2 eV above the valence-band maximum which should dominate the STM tunneling spectra. Finally, we have proposed a structural model for the C-rich $6\sqrt{3} \times 6\sqrt{3}$ phase.

[1] H. Morkoc, S. Strite, G. B. Gao, M. E. Lin, B. Sverdlov, and M. Burns, J. Appl. Phys. **76**, 1363 (1994).

[2] R. Kaplan, Surf. Sci. **215**, 111 (1989).

[3] J. M. Nicholls, B. Reihl, and J. E. Northrup, Phys. Rev. B **35**, 4137 (1987); J. E. Northrup, Phys. Rev. Lett. **57**, 154 (1986); **53**, 683 (1984).

[4] C. S. Chang, I. S. T. Tsong, Y. C. Wang, and R. F. Davis, Surf. Sci. **256**, 354 (1991).

[5] F. Owman and P. Martensson, Surf. Sci. **330**, L639 (1995).

[6] J. P. Perdew and A. Zunger, Phys. Rev. B **23**, 5048 (1981).

[7] R. Stumpf and M. Scheffler, Comput. Phys. Commun. **79**, 447 (1994).

[8] L. Kleinman and D. Bylander, Phys. Rev. Lett. **48**, 1425 (1982).

[9] N. Troullier and J. L. Martins, Phys. Rev. B **43**, 1993 (1991). For the C pseudopotential these authors employed $r_{cs} = 1.50 a_B$ and $r_{cp} = 1.54 a_B$, where $a_B = 0.529$ Å.

[10] X. Gonze, R. Stumpf, and M. Scheffler, Phys. Rev. B **44**, 8503 (1991).

[11] G. X. Qian, R. M. Martin, and D. J. Chadi, Phys. Rev. B **38**, 7649 (1988).

[12] J. E. Northrup and S. Froyen, Phys. Rev. Lett. **71**, 2276 (1993).

[13] O. Kubaschewski and C. B. Alcock, *Metallurgical Thermochemistry* (Pergamon, Oxford, 1979).

[14] *Semiconductors: Group IV Elements and III-V Compounds*, edited by O. Madelung (Springer-Verlag, Berlin, 1991).

[15] T. Kinoshita, S. Kono, and T. Sagawa, Phys. Rev. B **34**, 3011 (1986).

[16] R. G. Wyckoff, *Crystal Structures* (Wiley, New York, 1975).